

# Pharmacological Characterization of a Novel Nonpeptide Antagonist for Formyl Peptide Receptor-Like 1<sup>§</sup>

Caihong Zhou, Song Zhang, Masakatsu Nanamori, Yueyun Zhang, Qing Liu, Na Li, Meiling Sun, Jun Tian, Patrick P. Ye, Ni Cheng, Richard D. Ye, and Ming-Wei Wang

The National Center for Drug Screening, Shanghai Institute of Materia Medica (C.Z., Y.Z., Q.L., N.L., M.S., M.-W.W.), and the Graduate School (S.Z.), Chinese Academy of Sciences, Shanghai, China; and Department of Pharmacology, College of Medicine, University of Illinois, Chicago, Illinois (M.N., J.T., P.P.Y., N.C., R.D.Y.)

Received April 27, 2007; accepted July 25, 2007

## ABSTRACT

A series of quinazolinone derivatives were synthesized based on a hit compound identified from a high-throughput screening campaign targeting the human formyl peptide receptor-like 1 (FPRL1). Based on structure-activity relationship analysis, we found that substitution on the *para* position of the 2-phenyl group of the quinazolinone backbone could alter the pharmacological properties of the compound. The methoxyl substitution produced an agonist 4-butoxy-N-[2-(4-methoxy-phenyl)-4-oxo-1,4-dihydro-2*H*-quinazolin-3-yl]-benzamide (Quin-C1; C1), whereas a hydroxyl substitution resulted in a pure antagonist, Quin-C7 (C7). Several partial agonists were derived from other substitutions on the *para* position. C7 partially displaced [<sup>125</sup>I]Trp-Lys-Tyr-Met-Val-*D*-Met-NH<sub>2</sub> (WKYMVm) binding to FPRL1 but not [<sup>3</sup>H]*N*-formyl-Met-Leu-Phe to formyl peptide receptor. In functional assays using FPRL1-expressing RBL-2H3 cells, C7 inhibited calcium mobilization and chemotaxis induced by WKYMVm and C1 and degranulation elicited by C1. C7 also suppressed C1-induced extracellular signal-regulated kinase phosphorylation and reduced arachidonic acid-induced ear edema in mice. This study represents the first characterization of a nonpeptidic antagonist for FPRL1 and suggests the prospect of using low molecular weight compounds as modulators of chemoattractant receptors *in vitro* and *in vivo*.

The human formyl peptide receptor (FPR) family of chemoattractant receptors consists of FPR, formyl peptide receptor-like 1 (FPRL1), and FPRL2. These receptors are expressed primarily in neutrophils and monocytes and exert important functions in inflammation and immunity (Le et al., 2002). The FPRL1 gene was initially cloned in 1992 for its homology with FPR cDNA (Bao et al., 1992; Murphy et al., 1992; Ye et al., 1992). The prototype of chemoatactic peptide *N*-formyl-Met-Leu-Phe (fMLF), an agonist for FPR, can also

activate FPRL1 with a reduced affinity (Quehenberger et al., 1993). Stimulation of FPRL1 elicits a cascade of host defense reactions against pathogens, including chemotaxis, superoxide generation, and exocytosis in human neutrophils. In addition, it was reported that FPRL1 attenuates HIV-1 infection by desensitizing and down-regulating the chemokine receptors CCR5 and CXCR4, which serve as major coreceptors for HIV-1, on monocyte surfaces (Li et al., 2001). A recent study showed that the expression of FPRL1 in mouse C26 cells markedly reduced tumorigenicity in syngeneic mice and resulted in high levels of humoral immune response to both FPRL1-containing and wild-type C26 cells (Hu et al., 2005). The data indicate that FPRL1 also plays a key role in specific antitumor response. The expression of FPRL1 in activated microglial cells and its function as a receptor for Abeta(1–42), a 42-amino acid form of the beta-amyloid peptide, suggest that FPRL1 is closely related to neurodegenerative disorders (Hu et al., 2005). Investigation in ligand binding, signal transduction, and functional properties of FPRL1 is expected to facilitate

This project was supported in part by grants from the Ministry of Science and Technology of China (2004CB518902 to M.-W.W.), Chinese Academy of Sciences (KSCX1-SW-11-2 to M.-W.W.), Shanghai Municipality Science and Technology Development Fund (05DZ22914 and 06DZ22907 to M.-W.W.), and National Institutes of Health (AI033503 to R.D.Y.).

C.Z. and S.Z. contributed equally to this work.

Article copyright date and citation information can be found at <http://molpharm.aspetjournals.org>.  
doi:10.1124/mol.107.037564

<sup>§</sup> The online version of this article (available at <http://molpharm.aspetjournals.org>) contains supplemental material.

**ABBREVIATIONS:** FPR, formyl peptide receptor; FPRL1, formyl peptide receptor-like 1; SAR, structure-activity relationship; HTS, high-throughput screening; WKYMVm, Trp-Lys-Tyr-Met-Val-*D*-Met-NH<sub>2</sub>; fMLF, *N*-formyl-Met-Leu-Phe; DMEM, Dulbecco's modified Eagle's medium; FBS, fetal bovine serum; BSA, bovine serum albumin; NF- $\kappa$ B, nuclear factor- $\kappa$ B; ERK, extracellular signal-regulated kinase; DMSO, dimethyl sulfoxide; AA, arachidonic acid; GPCR, G protein-coupled receptor; HIV-1, human immunodeficiency virus-1; Quin-C1, 4-butoxy-*N*-(2-(4-methoxy-phenyl)-4-oxo-1,4-dihydro-2*H*-quinazolin-3-yl)-benzamide.

iate the understanding of this receptor as a new therapeutic target.

Among the FPR family of receptors, FPRL1 has the broadest spectrum of ligands (Migeotte et al., 2006). Except for one lipid (lipoxin A4), all identified FPRL1 ligands are small peptides and include host-derived agonist LL-37, natural or synthetic peptides (humanin, MMK-1, and WKYMVm), and peptides derived from HIV-1 envelope proteins (Le et al., 1999; Yang et al., 2000). These pharmacological properties of FPRL1 imply that it is a potential target for therapeutic intervention. However, identification of antagonists for this receptor has met with difficulties. A new peptide (WRW-WWW; WRW<sup>4</sup>) has been identified as an antagonist for FPRL1 by screening a hexapeptide library (Bae et al., 2003). Because of inherent limitations of peptides as therapeutic agents, it is desirable to develop synthetic, nonpeptidic ligands for receptors. Not long ago, we initiated a high-throughput screening (HTS) campaign to identify FPRL1 ligands from a synthetic compound library. After vigorous screening and structure modification, a substituted quinazolinone compound (Quin-C1; 4-butoxy-N-[2-(4-methoxy-phenyl)-4-oxo-1,4-dihydro-2H-quinazolin-3-yl]-benzamide) was discovered. This compound (C1) displayed selective agonistic effects on FPRL1 (Nanamori et al., 2004). As an ongoing effort to study the structure-activity relationship (SAR) of the original compound, we designed, synthesized, and characterized a series of substituted quinazolinone derivatives as modulating agents for FPRL1. Our results indicate that a hydroxyl substitution on the *para* position of the 2-phenyl group of the quinazolinone backbone resulted in a pure antagonist, Quin-C7 (C7), which displayed inhibitory effects on FPRL1.

## Materials and Methods

**Materials.** WKYMVm was synthesized at GL Biochem (Shanghai) Ltd. (Shanghai, China). WRW<sup>4</sup> and MMK-1 were made at HD Biosciences Co. (Shanghai, China). <sup>125</sup>I-WKYMVm (Bolton-Hunter-labeled), [<sup>3</sup>H]MLF, and FlashBlue GPCR scintillating beads were obtained from PerkinElmer Life and Analytical Sciences (Waltham, MA). Steady-Glo Luciferase Assay Solutions were purchased from Promega Corporation (Madison, WI). Fluoro-4/acetoxymethyl ester, Dulbecco's modified Eagle's medium (DMEM) culture medium, and trypsin were bought from Invitrogen (Carlsbad, CA). Fetal bovine serum (FBS) was purchased from HyClone Laboratories (Logan, UT). The anti-ERK1/2 and anti-phospho-ERK antibodies were procured from Cell Signaling Technologies (Danvers, MA). Other reagents were supplied by Sigma Chemical Co. (St. Louis, MO).

**Cell Culture.** The human cervical carcinoma cell line HeLa was transfected with pNF- $\kappa$ B-Luc reporter plasmid that contains five copies of NF- $\kappa$ B binding sequence (Stratagene, La Jolla, CA) and a human FPRL1 cDNA expression vector in pSFFV.neo vector as reported previously (Nanamori et al., 2004; Tian et al., 2005). The transfected cells were maintained in DMEM supplemented with 10% FBS. Rat basophilic leukemia cell line RBL-2H3 expressing either the human FPRL1 (RBL-FPRL1) or human FPR (RBL-FPR) was described previously and was maintained in DMEM supplemented with 20% FBS (He et al., 2000).

**Compound Synthesis.** The quinazolinone series compounds were synthesized according to the method described previously (Mayer et al., 1997), and the synthetic route is shown in Fig. 1. Anthranilic acid derivative 5 was obtained subsequently via reduction of compound 4 with zinc and acetic acid in  $\text{CH}_2\text{Cl}_2$ . Moderate to high yield was achieved through refluxing compound 5 with different substituted benzaldehydes in a mixed solvent ( $\text{CH}_2\text{Cl}_2/N,N$ -dimethyl-

ylacetamide catalyzed by acetic acid) using molecular sieve as dehydrating reagent.

**Ligand Binding Assay.** Ligand binding assay was performed as described previously (Yan et al., 2006). RBL-FPRL1 cells ( $\sim 10^6$ ) were harvested and washed twice with phosphate-buffered saline. Cell membrane was prepared with BioNeb Cell Disruption System (Glas-Col, Terre Haute, IN). Various concentrations of compounds were incubated together with RBL-FPRL1 cell membrane preparation, 0.16 nM [<sup>125</sup>I]WKYMVm (PerkinElmer Life and Analytical Sciences,  $K_{d} = 0.32 \text{ nM}$ ), and FlashBlue GPCR beads (100  $\mu\text{g}/\text{well}$ ) to give a final volume of 0.1 ml. The plates were incubated at 4°C for 12 h and centrifuged for 3 min at 2500g before counting on a MicroBeta scintillation counter (PerkinElmer Life and Analytical Sciences). To test the binding affinity for FPR, RBL-FPR cells ( $1 \times 10^6$ ) were seeded onto 24-well plates and incubated for 48 h. After being washed twice with blocking buffer (RPMI 1640 medium supplemented with 25 mM HEPES and 0.1% BSA, pH 7.5), cells were incubated with blocking buffer for 2 h and then sequentially with 30 nM [<sup>3</sup>H]MLF and different concentrations of C7 or unlabeled MLF in binding buffer (phosphate-buffered saline with 10% BSA) for another 2 h. Radioactivity was measured as above.

**Reporter Assay.** HeLa cells expressing NF- $\kappa$ B-Luc/FPRL1 (HeLa-kB-FPRL1) were seeded onto 96-well plates at a density of  $1.5 \times 10^4$  cells/well. After cells became adherent, they were serum-starved in DMEM for 16 h before screening assay. Different concentrations of compounds were added to the cells for 5 h, and the expressed luciferase activity was determined in an EnVision 2101 multilabel reader (PerkinElmer Life and Analytical Sciences) using the Steady-Glo Luciferase Assay solutions.

**Calcium Mobilization Assay.** Calcium mobilization assay was performed as described previously (Yan et al., 2006). In brief, RBL-FPRL1 cells were detached and collected by centrifugation, loaded with 5  $\mu\text{M}$  Fluo-4/AM (Invitrogen) in Hanks' balanced salt solution supplemented with 2.5 mM probenecid for 45 min, and then washed twice with Hanks' balanced salt solution. Cell suspensions were adjusted to a density of  $5 \times 10^6$  cells/ml and seeded onto 96-well plates (100  $\mu\text{l}/\text{well}$ ). Cells were reattached by centrifugation and then analyzed for calcium mobilization using FlexStation (Molecular Devices, Sunnyvale, CA) with excitation wavelength at 485 nm and emission wavelength at 525 nm. For antagonist mode, cells were incubated with or without test compounds for 15 min before the addition of WKYMVm (2 nM) or C1 (5  $\mu\text{M}$ ). For detailed characterization of RBL-FPRL1 cells, calcium mobilization assays were conducted on a spectrofluorometer (Photon Technology Inc., Lawrenceville, NJ), using Indo-1 as indicator and procedures described previously (Nanamori et al., 2004).

**Chemotaxis.** WKYMVm and C1-induced migration of cells was assayed in a 48-well microchemotaxis chamber (Neuro Probe, Cabin

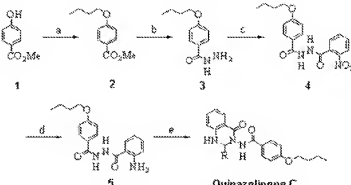


Fig. 1. The synthetic route of quinazolinone C. Reagents and conditions: a, 1: NaOH, MeOH, 0°C, 20 min; 2: n-BuLi, MeOH, reflux, 5 h; b,  $\text{N}_2\text{H}_4 \cdot \text{H}_2\text{O}$ , MeOH, reflux, 6 h; c, 2-nitrobenzoyl chloride,  $\text{Et}_3\text{N}$ ,  $\text{CH}_2\text{Cl}_2$ , 0°C to room temperature, overnight; d,  $\text{Zn}$ ,  $\text{AcOH}$ ,  $\text{CH}_2\text{Cl}_2$ , 0°C to room temperature, 4 h; e, substituted benzaldehyde,  $\text{AcOH}/\text{N,N}$ -dimethylacetamide/ $\text{CH}_2\text{Cl}_2$  (5:5:90), 4A molecular sieve, reflux, 12 h.

John, MA) as described previously (Nanamori et al., 2004). In brief, WKYMVm (10 nM, 30  $\mu$ l) or C1 (100 nM, 30  $\mu$ l) were placed in the lower chamber, and RBL-FPRL1 cells (50  $\mu$ l at  $1 \times 10^6$  cells/ml) were preincubated with or without test compounds for 15 min and then loaded in the upper chamber, which was separated from the lower chamber by a polycarbonate filter (pore size, 8  $\mu$ m). After incubation at 37°C for 4 h, the filter was removed, fixed, and stained with Diff-Quick staining solutions (IMEB Inc, San Marcos, CA). Chemotaxis was quantified by counting migrated cells in five randomly chosen high-power fields (400 $\times$ ).

**Phosphorylation of Mitogen-Activated Protein Kinases.** Activation of the p44/p42 mitogen-activated protein kinases (ERK1/2) was determined essentially as described previously (Nanamori et al., 2004). In brief, cells were cultured in six-well plates and serum-starved overnight before agonist stimulation. Some samples were pretreated with the antagonist (C7) for 15 min before agonist (C1) stimulation for 5 min. The reaction was terminated by adding 300  $\mu$ l of ice-cold SDS-polyacrylamide gel electrophoresis loading buffer [15% (v/v) glycerol, 125 mM Tris-Cl, pH 6.8, 5 mM EDTA, 2% (w/v) SDS, 0.1% bromophenol blue, and 1%  $\beta$ -mercaptoethanol]. Samples were sonicated to disperse DNA contents. After boiling, samples were analyzed by SDS-polyacrylamide gel electrophoresis and Western blot using anti-ERK1/2 and anti-phospho-ERK2 antibodies at 1:1000 dilution. Horseradish peroxidase-conjugated anti-rabbit antibody (1:3000) was used as secondary antibody. The resulting immunocomplex was visualized by SuperSignal West Pico Chemiluminescence (Pierce, Rockford, IL).

**Ear Edema Assay.** Male BALB/c mice weighing 20 to 24 g (Shanghai SLAC Laboratory Animals Co., Shanghai, China) were used in the experiment. The animals were housed in an environmentally (25°C) and air humidity (60%) controlled room with a 12-h light/dark cycle and kept on a standard laboratory diet and drinking water ad libitum. Mice were fasted for 18 h with free access to water and divided into groups of four to seven animals. The study was conducted according to the procedures approved by the institutional animal care committee.

Inflammation was induced by arachidonic acid (AA) as described previously with minor modifications (Rao et al., 1993). In brief, AA (0.25 mg in 20  $\mu$ l of 5% DMSO and 95% acetone) was topically applied onto both surfaces of the right ear of each mouse. Left ear (control) received solvent treatment. C7, at various doses dissolved in 1% DMSO, 19% polyethylene glycol 400, and 80% normal saline, was administered intraperitoneally (200  $\mu$ l) 0.5 h before AA application. Two control groups were used: one was treated with vehicle, and the other received dexamethasone (1 mg). Inflammation was induced for 3 h after AA application, and the animals were sacrificed by cervical dislocation. An 8-mm section from each ear was removed with a metal punch and weighed immediately. Ear edema was determined by subtracting the weight of the left ear from that of the right ear. The rate of edema (percentage) was calculated by dividing the weight difference between the left and right ear with the left ear weight and multiplied by 100.

## Results

**Characterization of Quinazolinone Derivatives as FPRL1 Ligands.** In a previous study, we conducted an HTS of 15,760 synthetic and 400 natural compounds. Among these, three compounds were found to be potential FPRL1 agonists. Based on one hit compound, whose core structure is shown in Fig. 2A, we developed the first nonpeptidic ligand Quin-C1 for FPRL1 (Nanamori et al., 2004). To search for FPRL1 antagonists, four series of quinazolinone derivatives (C, M, W, and O) were synthesized (Fig. 2A). Few compounds in the M, W, and O series showed activity. The preliminary SAR analysis of C series compounds indicated that the substitution of the phenyl group at the 2 position of quinazolinone

one backbone might be a possible determinant for its functional property. Thus, more derivatives of C series were made (Fig. 2B) in accordance with the method described previously (Mayer et al., 1997). Amino-substituted compound (C11) was obtained by reduction of its corresponding nitro substituted compound (C10).

To determine the substituted position, four compounds were synthesized first. There was a methoxy group at the 4' position in C1 and a 2',4'-disubstitution in C2 and C4. C6 contains no substitution in the aromatic ring. These modifications produced drastically different effects: among these compounds, C2, C4, and C6 lost agonist activity entirely in the calcium mobilization assay (Supplementary Fig. S1). However, C1 showed a stronger agonist activity than that of the hit compound (Table 1).

Next, compounds with different substitutions at the 4' position were synthesized to study the impacts of the substituted groups. C1 (4'-methoxy), C5 (4'-methyl), and C10 (4'-nitro) exhibited strong agonist activity (Table 1). Substitutions with bulky groups, such as isobutoxy (C9) or n-butoxy (C12), resulted in decreased or loss of bioactivity. Bioactivity also decreased when the nitro was changed to amino (C11) and lost when changed to *N,N*-dimethylamino group (C3). Of particular interest is the complete reversal of bioactivity when the methoxy group was substituted with a hydroxyl

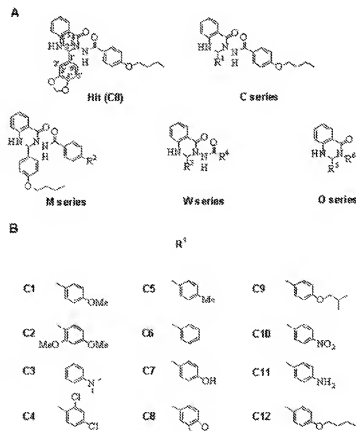


**Fig. 2.** Chemical structures of hit compound (C8) and its derivatives. A, structure of the hit compound identified from high-throughput screening and its four series derivatives (C, M, W, and O). B, structures of C series derivatives at R<sup>1</sup>. Compound C1 is the previously reported FPRL1 agonist Quin-C1. Derivatives were designed based on hit compound C8 by changing the substitution on the phenyl group at the 2 position while keeping the basic quinazolinone skeleton.

group (C7). This substitution resulted in an antagonist for FPRL1 (see below).

**C7 Inhibits WKYVM<sub>n</sub>-Stimulated Calcium Mobilization.** Although C7 showed a higher binding affinity than C9, which exhibited bioactivity in reporter assay, no agonist activity was detected in both reporter and calcium mobilization assays (Table 1). Because the reporter assay involves the activation of several signaling pathways and is distal from the receptor, we conducted additional studies to study the proximal signaling events induced by the activated receptor. Further characterization was conducted with C7 and C12 in calcium mobilization assays. Calcium mobilization results from FPRL1-activated PLC $\beta$ , which generates the second messengers diacyl glycerol and inositol 1,4,5-trisphosphate. The RBL-FPRL1 cell line, used in this and other functional studies described in this article, was generated through stable expression of the human FPRL1 cDNA. Reverse transcription-polymerase chain reaction analysis showed that it does not contain transcript for human FPR and FPRL2 (Fig. 3A). In calcium mobilization assays (Fig. 3B), the cell line responded strongly to WKYVM<sub>n</sub> (100 nM); it responded to C1 at a higher concentration (100  $\mu$ M) but was sensitive to the FPRL1-selective agonist MMK1 (100 nM). However, RBL-FPRL1 only weakly responded to fMLF (100 nM), a high-affinity agonist for FPR and low-affinity agonist for FPRL1. F2L, an agonist for FPRL2, did not induce calcium mobilization (data not shown). These results confirmed that the observed calcium mobilization was mediated by FPRL1 but not the structurally related FPR or FPRL2. As shown in Fig. 4, C7 antagonized WKYVM<sub>n</sub>-stimulated calcium mobilization in a dose-dependent manner, whereas C12 inhibited WKYVM<sub>n</sub>-stimulated calcium mobilization no more than 20% at concentrations up to 100  $\mu$ M.

**C7 Suppresses Chemotaxis in C1 and WKYVM<sub>n</sub>-Stimulated RBL-FPRL1 Cells.** In chemotaxis assay, C7 inhibited C1-induced cell migration in a dose-dependent manner (Fig. 5). Given the structural similarity between these two compounds, the antagonistic effect was expected. It is interesting that C7 also suppressed chemotaxis induced by WKYVM<sub>n</sub>, a highly potent FPRL1 agonist with no structural resemblance to C7. Our earlier study suggested a partial overlap between C1 and WKYVM<sub>n</sub> in FPRL1 binding (Nanamori et al., 2004). The data shown in Fig. 5 could be partially explained with the homologous structures of C7 and

C1. Our results also indicate that C7 could reduce WKYVM<sub>n</sub>-stimulated degranulation by up to 57% (data not shown) and C1-induced degranulation in a dose-dependent manner (Supplement Fig. S2) in RBL-FPRL1 cells.

**C7 and Its Analogs Compete with WKYVM<sub>n</sub> for Binding to RBL-FPRL1 Cells.** To study the binding properties of C7 and other C series compounds to FPRL1, competitive binding assays using [<sup>125</sup>I]WKYVM<sub>n</sub> were performed with membranes prepared from RBL-FPRL1 cells. C7 and selected analogs competed effectively for binding to RBL-FPRL1 (Fig. 6). Among the analogs studied, C1 and C5 are more potent than C7, exhibiting IC<sub>50</sub> values of 92  $\pm$  1 and 174  $\pm$  61 nM, respectively. C7 could not completely displace [<sup>125</sup>I]WKYVM<sub>n</sub> binding to FPRL1 at 100  $\mu$ M, the highest concentration used in the assay because of limited solubility of the compound. The IC<sub>50</sub> value of 6653  $\pm$  859 nM (Table 1) was derived from maximal but not complete displacement of the radioligand. Although C7 is less potent than C1 in the competitive binding assay, it specifically interacts with FPRL1 but not FPR. In binding assays using FPR-transfected RBL cells, C7 at concentrations up to 100  $\mu$ M could not effectively compete with [<sup>3</sup>H]fMLF for binding to the RBL-FPR cells (Fig. 7).

**C7 Inhibits Agonist-Induced ERK Phosphorylation.** FPRL1-mediated activation of the mitogen-activated protein kinases, ERK1 and ERK2, was determined in C1-stimulated RBL-FPRL1 cells based on activation-associated phosphorylation (Payne et al., 1991). Maximal activation was observed at  $\sim$ 5 min after agonist stimulation. When the cells were pretreated with C7, the agonist-induced phosphorylation of ERK1 and ERK2 was reduced (Fig. 8). The inhibitory effect of C7 was evident at 3  $\mu$ M and higher. At 100  $\mu$ M, C7 reduced phosphorylated ERK to its base level.

**Comparing C7 with WRW<sup>4</sup> for Their Antagonistic Activities.** To date, WRW<sup>4</sup> is the only characterized peptide with selectivity for FPRL1 (Bae et al., 2004). The antagonistic effect of C7 was compared with that of WRW<sup>4</sup> in calcium mobilization assay. WKYVM<sub>n</sub>-induced calcium mobilization in RBL-FPRL1 cells was dose-dependently inhibited by C7 (Fig. 9A). Likewise, WRW<sup>4</sup> displayed inhibitory effect in the calcium mobilization assay (Fig. 9B). An analysis of the results demonstrated that C7 had antagonist efficacy (90.6%) comparable with that of WRW<sup>4</sup>, although its potency was not

TABLE 1

Bioactivities detected with the quinazolinone C derivatives

The compounds were evaluated for their binding abilities to FPRL1 in competition with [<sup>125</sup>I]WKYVM<sub>n</sub>. Agonist activities were assessed in HeLa cells stably transfected with human FPRL1 genes and a pNF-E2-Luc reporter plasmid. Calcium responses were examined in RBL-2H3 cells stably transfected with human FPRL1 genes (RBL-FPRL1). Efficacy was expressed as a percentage of the maximal response that elicited by 10  $\mu$ M (in the reporter assay) or 1  $\mu$ M (in the calcium mobilization assay) WKYVM<sub>n</sub>. Each value represents means  $\pm$  S.E.M. of three independent experiments.

Compound	FPRL1 Binding, IC <sub>50</sub>	Reporter Assay		Calcium Mobilization	
		EC <sub>50</sub> nM	Efficacy %	EC <sub>50</sub> $\mu$ M	Efficacy %
Hit (C8)	745 $\pm$ 104	472 $\pm$ 9	54.3 $\pm$ 0.1	12.34 $\pm$ 0.83	43 $\pm$ 3
C1	92 $\pm$ 1	15 $\pm$ 4	88.5 $\pm$ 9.1	0.47 $\pm$ 0.02	90 $\pm$ 4
C5	174 $\pm$ 61	46 $\pm$ 10	87.6 $\pm$ 5.0	1.48 $\pm$ 0.15	74 $\pm$ 4
C7	6653 $\pm$ 859	N.A.	N.A.	N.A.	N.A.
C9	>15,000	8064 $\pm$ 487	52.7 $\pm$ 4.2	N.A.	N.A.
C10	261 $\pm$ 59	89 $\pm$ 8	86.7 $\pm$ 11.5	1.10 $\pm$ 0.17	55 $\pm$ 3
C11	>15,000	1352 $\pm$ 201	31.1 $\pm$ 3.9	N.A.	N.A.
C12	>15,000	N.A.	N.A.	N.A.	N.A.
WKYVM <sub>n</sub>	0.4 $\pm$ 0.1	1.3 $\pm$ 0.2	100	0.0011 $\pm$ 0.0001	100

N.A., no activity (efficacy <15%, or potency >20  $\mu$ M).

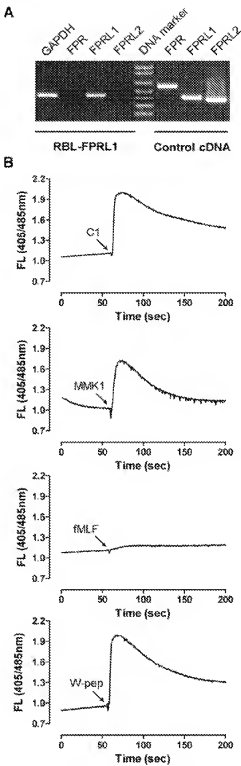


**Fig. 3.** Identification of FPRL1, but not FPR and PPRL2, in RBL-FPRL1 and characterization of its specificity. **A**, gel electrophoresis data showing polymerase chain reaction products obtained from RBL-FPRL1-derived cDNA. Only the FPRL1 transcript was detected. The specificity of the primers used is confirmed in reverse transcription-polymerase chain reaction using control cDNAs for human FPR1, FPRL1, and PPRL2. Polymerase chain reaction was conducted for 30 cycles. Glyceraldehyde-3-phosphate dehydrogenase was used as an internal control for the quality of the reverse-transcriptase product from RBL-FPRL1. **B**, calcium mobilization assay demonstrating the responsiveness of RBL-FPRL1 to C1 (100  $\mu$ M), WKYMVm (W-pep), the FPR1-selective peptide MMK1, and fMLF, a low-affinity peptide ligand for FPRL1. All peptide agonists were used at 100 nM. Representative tracings from three are shown.

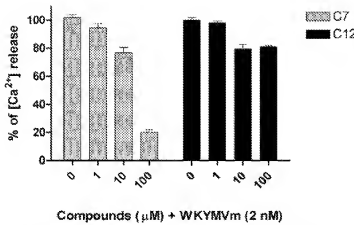


**Fig. 4.** Antagonist activity of compounds on WKYMVm-stimulated calcium mobilization. Different concentrations of C7 or C12 were added into RBL-FPRL1 cells 30 min before induction with 2 nM WKYMVm. The results (means  $\pm$  S.E.M.) are expressed as relative activity compared with the maximal  $[Ca^{2+}]$  release induced by 2 nM WKYMVm.

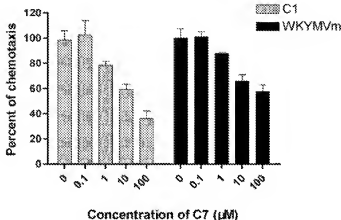


**Fig. 5.** Effects of C7 on C1 (100 nM) or WKYMVm (10 nM)-induced chemotaxis in RBL-FPRL1 cells. Various concentrations of C7 were added before the chemotaxis assay using C1 or WKYMVm as agonists. Data (means  $\pm$  S.E.M.) are expressed as a percentage of the maximal chemotaxis and are representative of two independent experiments.

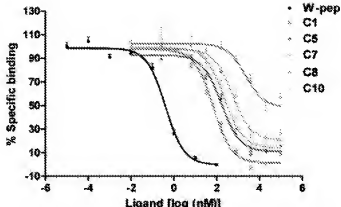


**Fig. 6.** Competitive binding of selected C series derivatives to  $[^{125}I]$ WKYMVm with FPRL1. Cell membrane was prepared from RBL-FPRL1 cells. Various concentrations of compounds were incubated together with RBL-FPRL1 cell membrane preparation, 0.16 nM  $[^{125}I]$ WKYMVm, and FlashBlue GPCR beads. The plates were incubated for 12 h and centrifuged for 3 min at 2500g before counting on a MicroBeta scintillation counter. The results (means  $\pm$  S.E.M.) are expressed as the percentage of specific binding from three independent experiments.

as good as WRW<sup>4</sup>. When C1 was used as agonist, the efficacy of C7 in the suppression of calcium release was similar to that of WRW<sup>4</sup> (65.9 versus 59.6%; Fig. 9, C and D).

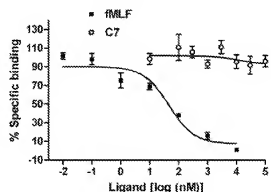
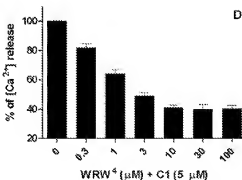
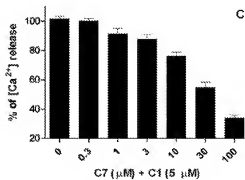
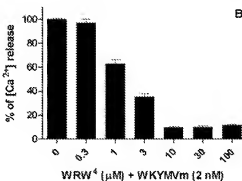
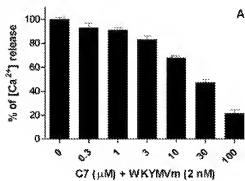


**Fig. 7.** Competitive binding of C7 with [<sup>3</sup>H]fMLF. RBL-FPR cells ( $1 \times 10^6$ ) were seeded onto 24-well plates and incubated for 48 h. After brief washing twice, cells were incubated with the blocking buffer (RPMI 1640 supplemented with 25 mM HEPES and 0.1% BSA, pH 7.5) for 2 h and then treated with different concentrations of C7 or unlabeled fMLF together with 30 nM [<sup>3</sup>H]fMLF for an additional 2 h. Radioactivity was measured by a MicroBeta scintillation counter. Data (means  $\pm$  S.E.M.) were collected from three to four independent experiments.



**Fig. 8.** Effects of C7 on C1-induced phosphorylation of ERK. RBL-FPR cells were pretreated with different concentrations of C7 or with vehicle control (DMSO of same concentration). After 15 min, the cells were stimulated with C1 (1 μM) for 5 min. Phosphorylation of ERK1 and ERK2 was determined as described under *Materials and Methods*. A representative set of blots is shown.



**C7 Inhibits Arachidonic Acid-Induced Ear Edema.** The in vivo effect of C7 was determined in an ear edema model (Rao et al., 1993). BALB/c mice were treated with AA (right ears) or solvent (left ears). In testing groups, different concentrations of C7 were given intraperitoneally to mice 0.5 h before AA application. A positive control group was included in which mice received dexamethasone instead of C7. Three hours later, animals were sacrificed, and ear edema was determined as described under *Materials and Methods*. As shown in Fig. 10, C7 dose-dependently inhibited AA-induced ear edema. At concentrations of 1 and 5 mg, the inhibitory effects of C7 approached that of dexamethasone (1 mg).

## Discussion

We reported previously the identification of Quin-C1 (C1), the first synthetic, nonpeptidic agonist for FPRL1 identified through an HTS campaign (Nanamori et al., 2004). Quin-C1 is one of the quinazolinone derivatives prepared from a core structure identified from 16,160 compounds. A preliminary SAR study suggests that substitutions at the 4' position of the 2-phenyl group of quinazolinone backbone play a key role for the bioactivity of the compounds, ranging from full agonists to full antagonists. These results indicate that small substitution groups at the 4' position can exhibit modulatory effects. In this study, we describe the functional characterization of Quin-C7 (C7), which contains a hydroxyl group at the 4' position and displays antagonistic effects in a variety of functional assays. In competitive binding assays, C7 showed binding affinity for FPRL1 lower than that of C1, C5, and C10 but higher than the binding affinities of C9, C11, and C12. This binding property is highly selective for FPRL1 because it did not compete the interaction between FPR and [<sup>3</sup>H]fMLF (Fig. 7). It is notable that C7 was unable to com-

**Fig. 9.** Antagonistic activity of C7 on WKYMVm or C1-stimulated calcium mobilization. WRW<sup>4</sup> was used as a control. Different concentrations of C7 or WRW<sup>4</sup> were added into RBL-FPR cells 30 min before induction with 2 nM WKYMVm (A and B) or 5 μM C1 (C and D). Data are expressed as relative activity compared with the maximal [Ca<sup>2+</sup>] release induced by 2 nM WKYMVm or 5 μM C1. Results were means  $\pm$  S.E.M. of three independent experiments.

pletely displace [ $^{125}\text{I}$ ]WKYMVm in competitive binding assays. Because of the limitation of its solubility, C7 could not be used for more than 100  $\mu\text{M}$  in our assays. The binding data suggest that C7 is a partial antagonist for WKYMVm binding to FPRL1. As discussed below, WKYMVm and C7 may occupy partially overlapping binding sites on FPRL1 because of the difference in their structures. The fact that C7 was more effective in the inhibition of C1-induced than WKYMVm-induced responses (Figs. 8 and 9) clearly reflects the structural similarities between C7 and C1. As shown in Fig. 4, the inhibitory effect of C7 is specific for FPRL1 and not caused by cytotoxicity, because C12, a compound of the same structural group, was neither toxic nor bioactive when tested in the same system. Moreover, the RBL-FPRL1 cell line used in this study was an engineered cell line that expresses human FPRL1 but not human FPR or FPRL2 (Fig. 3A). The selectivity of the cell line was confirmed in calcium mobilization assays, which displayed pharmacological properties of FPRL1 with functional responses to MMK1 and WKYMVm but only weakly to fMLF (Fig. 3B). Together, our data support the conclusion that C7 is a selective antagonist for FPRL1. Our attempt to generate an RBL cell line expressing human FPRL2 was not successful, probably because of the reported tendency of this receptor to express intracellularly (Migeotte et al., 2006). Therefore, the possibility that C7 acts on FPRL2 cannot be ruled out at this time.

The binding pockets of FPRL1 for its ligands have not been fully characterized. Based on the broad spectrum of ligand specificity, it is predicted that multiple binding sites exist in FPRL1 that allow its interaction with both peptides (e.g., A $\beta_{1-42}$ , MMK-1, SAA) and a lipid (lipoxin A<sub>2</sub>). Our previous characterization revealed a partial interference between WKYMVm and C1 in binding assays (Nanamori et al., 2004). This may result from a partial overlap of the two binding sites or an allosteric effect of one ligand that alters the binding of the other ligand. The C series compounds characterized in this work are derivatives of C1, and they probably share the same binding site with C1. The observation that C6, which contains no substitutions in the phenol ring and lost its bioactivity in the calcium mobilization assay, suggests that small substitution groups at the 4' position are critical

to the function of the compounds. However, disubstitutions such as those in C2 and C4 and bulky substitutions such as the ones in C3 and C12 produced no bioactivity in the calcium mobilization assay. This latter finding indicates that the binding pocket for the C series compounds is relatively small and cannot accommodate bulky groups or disubstitutions. The observation that these compounds bound poorly to FPRL1 supports the notion that a part of the binding pocket for the C series compounds provides very limited space.

Our preliminary SAR study also points to the importance for proper contact between the small substitution group at the 4' position and the receptor's binding site. Such an interaction is crucial to the bioactivity of the compounds. Small substitution groups such as the methoxy, methyl, and nitro groups are excellent for the agonistic activity, whereas a larger substitution group in C8 may be responsible for the reduced agonistic activity. Relative potency, both agonistic and antagonistic, may also require proper spacing between the contact sites such that compounds with an oxygen placed at the 4' position of the phenol ring (C1 and C7) proves to be most efficacious. However, C9 and C12 are much less effective probably because of the larger size of the substitution groups.

Chemoattractant receptors play a key role in the regulation of short- and long-term inflammation. In this study, we have shown that C7 effectively inhibited AA-induced ear edema, suggesting an in vivo effect of C7 in the suppression of inflammation. Several possibilities exist for this anti-inflammatory effect. First, C7 suppresses AA-induced ear edema through a blockade of FPRL1, offsetting the proinflammatory effect of a FPRL1 agonist released by AA-treated cells. Supporting this possibility is our *in vitro* result indicating C7 as a selective antagonist for FPRL1. However, the exact agonist(s) produced by AA-stimulated cells are not known at present, because FPRL1 has a particularly broad ligand selectivity and can respond to a variety of proinflammatory peptides (Migeotte et al., 2006). Second, C7 directly acts on FPRL1 as an anti-inflammatory ligand in a manner similar to that of lipoxin A4. There are indeed similarities between the two agents because neither was able to perform like a typical agonist yet exhibited anti-inflammatory properties. The mechanism underlying the anti-inflammatory effect of lipoxin A4 has not been fully understood, but induction of suppressor of cytokine signaling 2 was shown to contribute to this effect (Machado et al., 2006). It would be interesting to determine whether C7 can also induce suppressor of cytokine signaling 2. Finally, it remains a possibility that C7 acts on a target molecule other than FPRL1. Although there is no direct evidence supporting the presence of another C7 target, the fact that C7 can reduce ear edema as effectively as dexamethasone is of interest and suggests the potential of developing an anti-inflammatory agent based on this lead compound.

As one of the primary chemoattractant receptors in neutrophils and monocytes, FPRL1 has a particularly broad ligand selectivity. However, progress has been slow in the identification of its antagonist. WRW<sup>4</sup> was the first peptidic antagonist specifically targeting FPRL1, and its potency for maximal antagonism in the low micromolar range is reasonably good. Although C7 was approximately 36- to 50-fold less potent than WRW<sup>4</sup> in similar functional assays, it could attain comparable suppression efficacy in the calcium mobi-

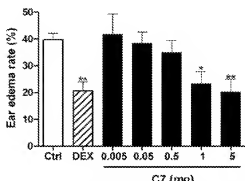


**Fig. 10.** Inhibition of arachidonic acid-induced ear edema by C7. BALB/c mice were treated intraperitoneally with vehicle (1% DMSO, 19% polyethylene glycol 400, and 80% normal saline; Ctrl), dexamethasone (DEX, 1 mg), or various concentrations of C7 30 min before application of AA (0.25 mg in 20  $\mu\text{l}$  of a solution containing 5% DMSO and 95% acetone). Three hours later, ear edema was determined as described under *Materials and Methods* and expressed as ear edema rate. Data shown are means  $\pm$  S.E.M. based on one experiment with four to seven mice in each group.

lization assay in RBL-FPRL1 cells. The current study suggests the possibility of improving its efficacy with further structural modifications.

#### Acknowledgments

We thank Drs. Guangxing Wang and Dale E. Mais for valuable discussions and Pangke Yan, Qinghai Tian, Xiaozhen Cheng, Huili Lu, and Zhen Zhang for technical assistance.

#### References

Bae YS, Lee HY, Je EJ, Kim JI, Kang HK, Ye RD, Kwak JY, and Ryu SH (2004) Identification of peptides that antagonize formyl peptide receptor-like 1-mediated signaling. *J Immunol* **173**:607–614.

Bae YS, Ye RD, Lee HY, Je EJ, Kim JI, Lee TG, Ye RD, Kwak JY, and Ryu SH (2003) Differential activation of formyl peptide receptor-like 1 by peptide ligands. *J Immunol* **171**:6807–6812.

Bao L, Gerard NP, Eddy RL, Shows TB, and Gerard C (1992) Mapping genes for the human C5a receptor (C5AR), human FMLP receptor (FPRL) and two FMLP receptor homologous orphan receptors (FPRL1, FPRL2) to chromosome 19. *Genomics* **13**:407–440.

He R, Tan L, Browning DD, Wang JM, and Ye RD (2000) The synthetic peptide Trp-Lys-Tyr-Met-Val-D-Met is a potent chemoattractant agonist for mouse formyl peptide receptor. *J Immunol* **165**:4598–4605.

Hu J, Li G, Tong Y, Li Y, Zhou G, He X, Xie P, Wang JM, and Sun Q (2005) Transcription of the gene encoding for a human G-protein coupled receptor FPRL1 in mouse tumor cells increases host anti-tumor immunity. *Int Immunopharmacol* **5**:971–980.

Le Y, Gong W, Li B, Dunlop NM, Shen W, Su SB, Ye RD, and Wang JM (1999) Utilization of two seven-transmembrane, G protein-coupled receptors, formyl peptide receptor-like 1 and formyl peptide receptor, by the synthetic hexapeptide WKYMVm for human phagocyte activation. *J Immunol* **163**:6777–6784.

Le Y, Murphy PM, and Wang JM (2002) Formyl-peptide receptors revisited. *Trends Immunol* **23**:541–548.

Le D, Hwang I, Scott JA, Henderson EB, Rogers TJ, Gong W, Le Y, Russetti FW, and Wang JM (2001) The synthetic peptide WKYMVm attenuates the function of the chemokine receptors CXCR2 and CXCR4 through activation of formyl peptide receptor-like 1. *Blood* **97**:2341–2347.

Machado FS, Johnstone JE, Eaper L, Dias A, Basica A, Serban CN, and Aliberti J (2006) Anti-inflammatory actions of lipoxin A4 and aspirin-triggered lipoxin are SOCS2 dependent. *Nat Med* **12**:330–334.

Mayer JP, Lewis GS, Curtis MJ, and Zhang J (1997) Solid phase synthesis of quinazolinones. *Tetrahedron Lett* **38**:8445–8448.

Migeotte I, Communi D, and Parmentier M (2006) Formyl peptide receptors: a promiscuous subfamily of G protein-coupled receptors controlling immune responses. *Cytokine Growth Factor Rev* **17**:501–519.

Murphy PM, Ozcelik T, Kenney RT, Tiffany HL, McDermott D, and Francke U (1992) A structural homologue of the N-formyl peptide receptor: Characterization and chemoattractant mapping of a peptide chemoattractant receptor family. *J Biol Chem* **267**:7697–7646.

Nanamori M, Cheng X, Mei J, Sang H, Xuan Y, Zhou C, Wang MW, and Ye RD (2004) A novel neuropeptide ligand for formyl peptide receptor-like 1. *Mol Pharmacol* **66**:1213–1222.

Payne DM, Rossmannino AJ, Martino P, Erickson AK, Her JH, Shabankhani J, Hunt DF, Weber MJ, and Sturgill TW (1991) Identification of the regulatory phosphorylation sites in pp42/mitogen-activated protein kinase (MAP kinase). *EMBO J* **10**:885–892.

Quenkenberger O, Prossnitz ER, Cavanagh SL, Cochrane CG, and Ye RD (1993) Multiple domains of the N-formyl peptide receptor are required for high-affinity ligand binding. Construction and analysis of chimeric N-formyl peptide receptors. *J Biol Chem* **268**:18167–18175.

Rao S, Cava E, Kunkel AF, and Isacke PC (1993) Comparative evaluation of arachidonic acid (AA)- and 4-hydroxy-2-nonenal-phorbol acetate (TPA)-induced dermal inflammation. *Inflammation* **17**:723–741.

Tian Q, Li J, Xie X, Sun M, Sang H, Zhou C, An T, Hu L, Ye RD, and Wang MW (2005) Stereospecific induction of nuclear factor- $\kappa$ B activation by isoquinazolinones. *Mol Pharmacol* **68**:1534–1542.

Yang D, Chen Q, Schmidt AP, Anderson GM, Wang JM, Wooster J, Oppenheim JJ, and Chertow O (2000) IL-37, the neutrophil granule- and epithelial cell-derived cathelicidin, utilizes formyl peptide receptor-like 1 (FPRL1) as a receptor to chemoattract human peripheral blood neutrophils, monocytes, and T cells. *J Exp Med* **192**:1069–1074.

Yan P, Nanamori M, Sun M, Zhou C, Cheng N, Li N, Zheng W, Xiao L, Xie X, Ye RD, et al. (2006) The immunosuppressive cyclosporin A antagonizes human formyl peptide receptor through inhibition of euglobulin ligand binding. *J Immunol* **177**:7050–7058.

Ye RD, Cavanagh SL, Quenkenberger O, Prossnitz ER, and Cochrane CG (1992) Isolation of a cDNA that encodes a novel granulocyte N-formyl peptide receptor. *Biochem Biophys Res Commun* **184**:582–589.

**Address correspondence to:** Dr. Ming-Wei Wang, the National Center for Drug Screening, 189 Guo Shou Jing Road, Shanghai 201203, China. E-mail: mwwang@mail.shinc.ac.cn